

## Light storage on the time scale of a minute

Y. O. Dudin, L. Li, and A. Kuzmich

*School of Physics, Georgia Institute of Technology, Atlanta, Georgia 30332-0430, USA*

(Received 20 December 2012; published 6 March 2013)

Light storage on the minute scale is an important capability for future scalable quantum information networks spanning intercontinental distances. We employ an ultracold atomic gas confined in a one-dimensional optical lattice for long-term light storage. The differential ac Stark shift of the ground-level microwave transition used for storage is reduced to a sub-Hz level by the application of a magic-valued magnetic field. The  $1/e$  lifetime for storage of coherent states of light is prolonged up to 16 s by a microwave dynamic decoupling protocol.

DOI: [10.1103/PhysRevA.87.031801](https://doi.org/10.1103/PhysRevA.87.031801)

PACS number(s): 42.50.Gy, 32.10.Dk, 32.60.+i, 42.50.Dv

Achieving long atomic coherence lifetimes is of major importance for precision measurements, for simulation of model quantum systems, and for scalable quantum information networks. In particular, long-term storage of quantum states is a key ingredient for the distribution of entanglement over continental length scales  $L \sim 10^3$  km [1–5]. The latter involve entanglement that is generated locally and subsequently distributed by light transmission over optical fiber links or through free space. As direct entanglement distribution over optical fibers is limited by absorption to distances  $l \sim 100$  km, to distribute entanglement over longer distances the channel should be divided into multiple segments. Entanglement generated over these shorter segments is connected by performing joint quantum measurements at the intermediate locations, an approach known as the quantum repeater [1].

Several of the quantum repeater capabilities have already been demonstrated using ultracold atomic gases. Deterministic generation of single photons from an atomic ensemble using a repeated application of Raman scattering has been achieved, with millisecond-scale generation times [6,7]. Strong Rydberg interactions in a mesoscopic ensemble of a few hundred atoms have been employed for microsecond-scale deterministic single-photon generation [8]. Probabilistic Duan-Lukin-Circ-Zoller (DLCZ)-type [2] implementations of atom-light [9–11] and atom-atom [12] entanglement have been achieved. Long-term storage of single quantum excitations and conversion of quantum fields between storable and telecom wavelengths with efficiencies in excess of 60% and memory telecom light entanglement have been demonstrated [13,14].

Here we report the realization of light storage on the minute scale, achieved by confining an ultracold atomic gas in an optical lattice with a 3 min lifetime and employing magnetic compensation of differential light shifts and dynamic decoupling with microwave  $\pi$  pulses. The 16 s  $1/e$  lifetime is a significant advance over the value of  $\sim 0.3$  s for ultracold atoms in Refs. [15,16] and  $\sim 1$  s in a solid-state sample reported in Ref. [17].

The essential elements of the experimental setup are shown in Fig. 1. The atoms are initially loaded into a two-dimensional (2D) magneto-optical trap (MOT). A quadrupole magnetic field with a gradient of 18 G/cm perpendicular to the major trap axis is generated by two pairs of racetrack-shaped anti-Helmholtz coils. Two circularly polarized beams with an elliptical cross section are retroreflected such that the four beams are perpendicular to each other and to the major trap axis. The four beams and the 2D-quadrupole magnetic

field combine to transversely cool and compress the atoms. The trapping beams have a total power of 370 mW and are red-detuned 20 MHz from the  $5s_{1/2}, F = 2 \leftrightarrow 5p_{3/2}, F = 3$  transition, and a laser beam with 6.3 mW and that is locked to the  $5s_{1/2}, F = 1 \leftrightarrow 5p_{3/2}, F = 2$  transition in  $^{87}\text{Rb}$  is used as the repumper. A pair of linearly polarized, circularly shaped laser beams (the pushing beam and the retarding beam) are used for axial cooling, and to create a slow atomic beam to load a three-dimensional (3D)-MOT in the science chamber. Atom loading of the measured rate of  $9 \times 10^9$  s $^{-1}$  produces a 3D-MOT of more than  $10^{10}$  atoms in the science chamber in 1.2 s. Atoms loaded into the 3D-MOT undergo sub-Doppler cooling and are subsequently transferred into a one-dimensional (1D) optical lattice formed by interfering two 1064-nm yttrium aluminum garnet (YAG) laser beams intersecting at an angle  $\theta \approx 18^\circ$  in the horizontal plane. The two lattice beams have waists of 170  $\mu\text{m}$ , with a total power of 12.5 W, resulting in a maximum lattice depth of 78  $\mu\text{K}$ , with corresponding trap frequencies of (110,  $1.4 \times 10^4$ , 20) Hz in the ( $x, y, z$ ) dimension. After the cooling stage  $\sim 10^7$  atoms remain in the lattice. The cloud has longitudinal and transverse waists of 260 and 70  $\mu\text{m}$ . In the first 5 s, the atoms undergo a fast collisional decay. The decay of the upper ( $F = 2$ ) ground hyperfine level is considerably faster than that of the  $F = 1$  level due to the contribution of the hyperfine level-changing collisions, which expel atoms from the trap (Fig. 2). Therefore for light storage the atoms are optically pumped into the lower ( $F = 1$ ) hyperfine level after lattice loading.

The probe  $\Omega_p$  and control  $\Omega_c$  laser fields are resonant with the electronic transitions,  $|a\rangle \leftrightarrow |c\rangle$  and  $|b\rangle \leftrightarrow |c\rangle$  between levels  $|a\rangle = |5s_{1/2}, F = 1\rangle$ ,  $|b\rangle = |5s_{1/2}, F = 2\rangle$ , and  $|c\rangle = |5p_{1/2}, F = 1\rangle$ , as shown in the inset to Fig. 1. The two beam waists are 50 and 200  $\mu\text{m}$ , respectively. The group velocity of the probe field is strongly modified by the control field. The dynamics can be described in terms of a coupled light-matter excitation—the dark-state polariton [3]. The coupled excitation is converted into a pure excitation of the long-lived  $|a\rangle - |b\rangle$  atomic coherence when the control field is adiabatically switched off. The probe field has a full width at half maximum (FWHM) of 82 ns and peak power of 130 nW. The control field has a FWHM of 1040 ns and peak power of 160  $\mu\text{W}$ . After a storage period  $T_s$ , the control field retrieves the signal field. The latter is coupled to a single-mode fiber and directed onto an avalanche photodiode. The ratio of the pulse areas of the retrieved and incident probe field pulses determines the storage efficiency as a function

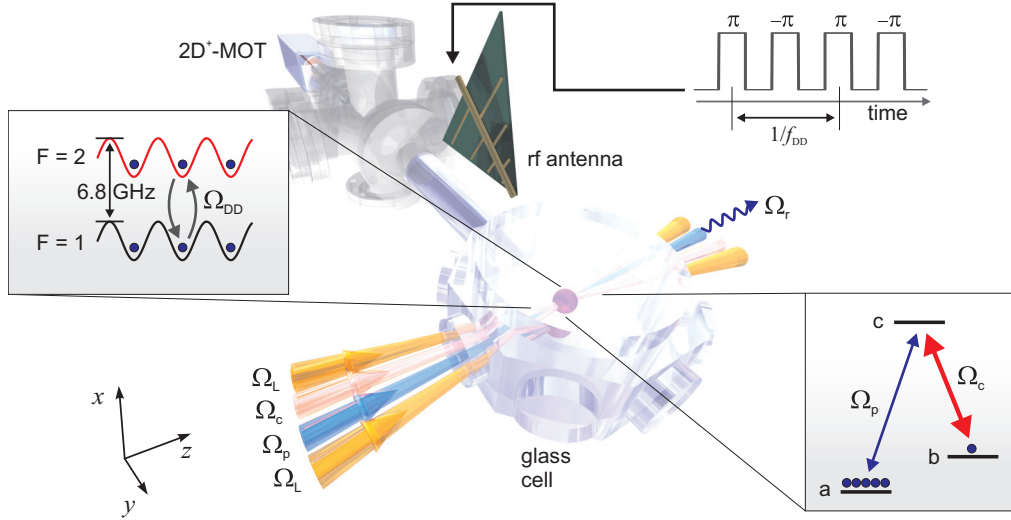


FIG. 1. (Color online) Essential elements of the experimental setup. A 2D-MOT produces a cold atomic beam to load a 3D-MOT in the differentially pumped glass cell with antireflection-coated windows. The 3D-MOT is used to produce a dense sample of cold  $^{87}\text{Rb}$  atoms in a 1D optical lattice formed by two 1064 nm  $\Omega_L$  fields. Atomic levels used in the experiment are shown in the inset. A probe pulse  $\Omega_p$  is converted into an atomic spin wave by adiabatically switching off the control field  $\Omega_c$ . After a storage period  $T_s$  the spin wave is retrieved into a phase-matched direction by turning the probe field back on. The lattice confines the atoms in the field maxima, minimizing spin-wave motional dephasing. The differential ac Stark shift produced by the lattice is nullified by setting the bias magnetic field to a “magic” value. A dynamic decoupling sequence of the microwave  $\pi$  pulses on the clock transition is used to extend storage time.

of storage period  $\eta(T_s)$ . To eliminate decoherence due to inhomogeneous magnetic fields, the  $(m_{F=1}, m_{F=2}) = (0, 0)$  ground-state atomic hyperfine coherence is used for storage. This so-called clock transition is magnetically insensitive, so that its energy depends only quadratically on external magnetic fields. We measured  $\eta(T_s = 1 \mu\text{s}) \approx 0.26$ .

The probe and control fields are aligned at an angle  $\approx 1.3^\circ$ , so the stored atomic excitation forms a spin wave  $\propto e^{i\Delta\vec{k}\cdot\vec{r}}$  of period  $\Lambda = 1/|\Delta\vec{k}| = 35 \mu\text{m}$ , where  $\Delta\vec{k} = \vec{k}_p - \vec{k}_c$  is the wave-vector mismatch between the probe and control fields. The thermal motion of atoms smears out the spin wave, limiting the storage lifetime. To minimize motional effects, we employ a 1D optical lattice of  $3.2 \mu\text{m}$  period that confines the atoms in the direction of the spin wave. We attribute a partial decay of retrieval efficiency on the time scale of tens of milliseconds

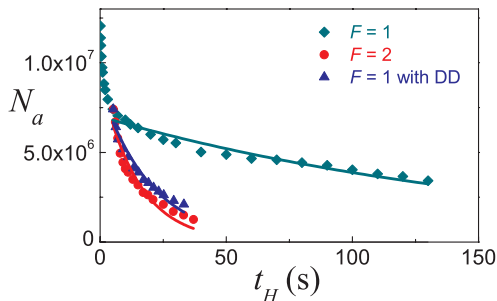


FIG. 2. (Color online) Number of lattice-trapped atoms  $N_a$  as a function of the holding time  $t_H$ . The data are for atoms prepared in  $5S_{1/2}, F = 1$  (diamonds),  $5S_{1/2}, F = 2$  (circles), and  $5S_{1/2}, F = 1$  when the dynamic decoupling sequence is applied (triangles). The data are fit with an exponential function  $\propto \exp(-t_H/\tau)$  starting from  $t_H = 5$  s, with the best-fit values of  $\tau = 169(14)$ ,  $15(1)$ , and  $20(1)$  s for atoms in  $F = 1$ ,  $F = 2$ , and  $F = 1$  with DD, respectively.

[measured  $\eta(T_s = 38 \text{ ms}) \approx 0.14$ ] to spin-wave dephasing due to atomic motion along the  $x$ - and  $z$ -lattice axes.

An unwanted byproduct of optical dipole trapping is that spatially separated atoms experience different ac Stark energy shifts caused by variations in the optical trapping field. The differential ac Stark shifts result in the dephasing of atomic coherences on millisecond time scales [7,18,19]. Dephasing which arises from inhomogeneous trapping potentials can be suppressed by introducing an additional light field that, together with the lattice light, is nearly two-photon resonant on a ladder transition [13], or by mixing the two ground hyperfine levels with a dc magnetic field in an elliptically polarized lattice at a particular (magic) magnetic field value [15,20]. Utilizing these techniques, the lifetime of light storage and quantum memory has been improved to  $\sim 0.3$  s [13–15].

To determine the “magic” magnetic field value, we measure the retrieved pulse energy as a function of the magnetic field, shown in the inset to Fig. 3. We use a Ramsey sequence of two  $\pi/2$  pulses to measure the quadratic magnetic shift of the clock transition to calibrate the value of the magnetic field. In addition to the clock coherence, we study storage with two other coherences that are weakly sensitive to magnetic field,  $(m_{F=1}, m_{F=2}) = (-1, 1)$  and  $(m_{F=1}, m_{F=2}) = (1, -1)$ . After loading, a bias magnetic field is applied along the major axis of the trap and atoms are either prepared in the  $5S_{1/2}, F = 1, m = 0$  state by means of optical pumping when clock coherence is addressed, or left unpolarized when  $(\pm 1, \mp 1)$  coherences are used. The polarization configurations of the probe and control fields are  $\text{lin}\perp\text{lin}$  for clock coherence and  $\sigma^\pm/\sigma^\mp$  for the  $(\mp 1, \pm 1)$  coherences. Gaussian fits of the data in the inset to Fig. 3 give  $B^{(0)} = 4.274(1)$ ,  $B^{(+)} = 5.431(2)$ , and  $B^{(-)} = 6.043(2)$  G for the three coherences, respectively. After correction by the degree of circular polarization of the two lattice beams  $A \equiv \sqrt{1 - \epsilon^2} = 0.990(6)$  [21] and by the geometrical

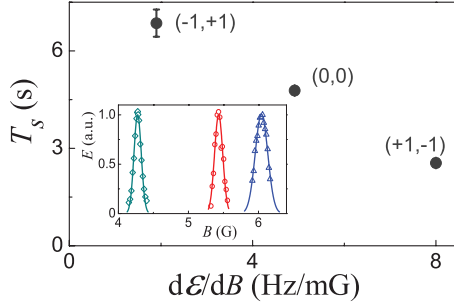


FIG. 3. (Color online) Measured light-storage lifetimes as a function of sensitivity to the magnetic field for three long-lived coherences. Error bars represent uncertainties from the exponential fits. The inset shows the retrieved pulse energy  $E$  as a function of the magnetic field. The pulse is retrieved after 5, 7, and 2 s for (0,0),  $(-1, 1)$ , and  $(1, -1)$  coherences, respectively. The Gaussian fits yield corresponding magic field values  $B^{(0)} = 4.27$ ,  $B^{(-)}$  = 5.43, and  $B^{(0)} = 6.04$  G.

factor  $\cos(\theta/2) \approx 0.988$ , we obtain the “magic” magnetic field values for the three coherences:  $B_0^{(0)} = 4.18(3)$  G,  $B_0^{(+)} = 5.31(3)$  G, and  $B_0^{(-)} = 5.91(4)$  G, respectively. These are in agreement, within the measurement errors, with the values found in Ref. [15]. It should be noted that in the latter the experiment was performed in a different apparatus, and it employed the Larmor precession of the stored spin waves for magnetic field calibration instead of the present microwave clock transition frequency measurement. Both Ref. [15] and the current work are in disagreement with the  $B_0^{(0)} \approx 4.38$  G theoretical prediction for our 1063.8 nm lattice [22].

The retrieved signal as a function of storage time taken at the “magic field” values for the three coherences is shown in Fig. 4. The observed decay can be ascribed to the spin-wave dephasing caused by the residual magnetic field combined with a weak first-order sensitivity of the used coherences to the magnetic field  $\mu' \equiv dE/dB$ . Here  $E$  is the energy of the corresponding hyperfine transition. The geometry of the vacuum setup was designed to minimize magnetic field

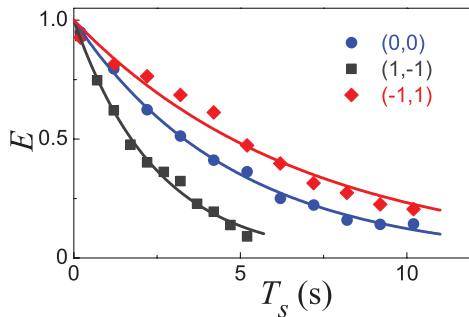


FIG. 4. (Color online) Retrieved pulse energy  $E$  as a function of storage time, normalized to its value at 38 ms, for the “magic” magnetic field values for the three long-lived coherences, (0,0) (circles),  $(-1, 1)$  (diamonds), and  $(1, -1)$  (squares). The storage efficiencies at 38 ms are 0.14, 0.06, and 0.05, respectively, for the three coherences. The solid lines are exponential fits to the data. The extracted  $1/e$  lifetimes are 4.8(1), 6.9(4), and 2.5(1) s for the clock,  $(-1, 1)$ , and  $(1, -1)$  transitions, respectively.

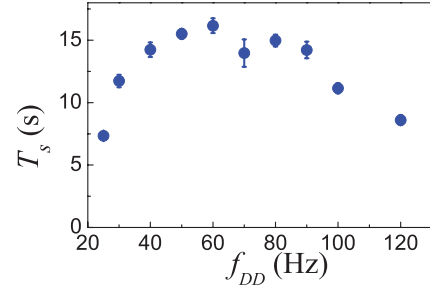


FIG. 5. (Color online) Lifetime as a function of the applied DD sequence frequency  $f_{DD}$ . The longest lifetime of 16 s is observed for  $f_{DD} = 60$  Hz. Higher  $f_{DD}$  result in lower lifetimes attributed to the accumulation of rotation errors.

gradients across the atomic cloud and was supplemented by magnetic field shielding. The longer 6.9 s lifetime is observed for the  $(-1, 1)$  coherence which has the lowest effective magnetic moment  $\mu'$ , whereas the lifetime of 2.5 s is measured for the  $(1, -1)$  coherence with the largest  $\mu'$  (Fig. 3).

To further extend the coherence time of the light storage, we apply a composite refocusing pulse sequence on the ground-level clock transition. Dynamic decoupling (DD) pulse sequences have been studied in great detail in the context of reducing the decoherence induced by external perturbations on the two-level system [23–29]. We apply the Carr-Purcell-Meiboom-Gill decoupling sequence [30] consisting of a train of resonant population-inverting microwave  $\pi$  pulses on the clock transition. The resonant 6.8 GHz field is generated by frequency mixing a 6.7 GHz output of a signal generator with a 100 MHz output of a direct digital synthesizer, which allows for fast and precise digital control of the microwave field phase by modulating the phase of the 100 MHz field. The 6 834 693 113 Hz frequency microwave field is calibrated to be in resonance with the clock transition by a Ramsey sequence of two  $\pi/2$  pulses. The same protocol is used for magnetic field calibration by measurements of the quadratic with a magnetic field shift of the clock transition frequency. The rf and microwave generators are locked to a Rb atomic frequency standard. The phase of the microwave field is alternated by  $180^\circ$  for two adjacent pulses to reduce the influence of pulse imperfections. The DD sequence suppresses decoherence that is slow compared to the decoupling frequency  $f_{DD} = 1/T_{DD}$ , where  $T_{DD}/2$  is the time interval between two

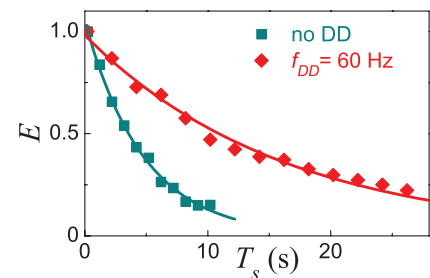


FIG. 6. (Color online) Retrieved pulse energy  $E$  as a function of storage time, normalized to its value at 38 ms, with (diamonds) and without (squares) the DD sequence applied. The solid curves are exponential fits.

consecutive pulses. For perfect  $180^\circ$  rotations the lifetime is generally expected to increase with  $f_{\text{DD}}$  [24,25].

The measured values of extended lifetimes are shown in Fig. 5. The maximum  $1/e$  lifetime of 16 s is measured for  $f_{\text{DD}} = 60$  Hz (Figs. 5 and 6). Retrieval efficiency  $\eta(T_s = 38 \text{ ms}) \approx 0.14$  is not affected by the DD pulse sequence for the used range of  $f_{\text{DD}}$ , but shorter lifetimes are observed for a higher  $f_{\text{DD}}$  (Fig. 5). This is attributed to the accumulation of rotation errors with an increased number of pulses. Atom loss also limits the maximum observed lifetime: With a DD sequence applied the atoms effectively spend half of the time in the relatively short-lived  $|5s_{1/2}, F = 2, m_F = 0\rangle$  state. The measured lifetime of the atoms in the trap when the DD

sequence is applied of 20 s (Fig. 2) provides an upper limit on storage lifetime.

In conclusion, by using atoms confined in a one-dimensional optical lattice with an ultralong trap lifetime and “magic” magnetic field to compensate the differential Stark shift and employing dynamic decoupling, we achieved storage of coherent states of light with a lifetime of 16 s.

We thank A. Marchenkova for laboratory assistance. This work was supported by the Air Force Office of Scientific Research Atomic Physics Program, Quantum Memories Multidisciplinary University Research Initiative, and National Science Foundation.

- 
- [1] H. J. Briegel, W. Dur, J. I. Cirac, and P. Zoller, *Phys. Rev. Lett.* **81**, 5932 (1998).
  - [2] L.-M. Duan, M. Lukin, J. I. Cirac, and P. Zoller, *Nature (London)* **414**, 413 (2001).
  - [3] M. Lukin, *Rev. Mod. Phys.* **75**, 457 (2003).
  - [4] L. H. Pedersen and K. Molmer, *Phys. Rev.* **79**, 012320 (2009).
  - [5] B. Zhao, M. Müller, K. Hammerer, and P. Zoller, *Phys. Rev. A* **81**, 052329 (2010).
  - [6] D. N. Matsukevich *et al.*, *Phys. Rev. Lett.* **97**, 013601 (2006).
  - [7] R. Zhao *et al.*, *Nat. Phys.* **5**, 100 (2009).
  - [8] Y. O. Dudin and A. Kuzmich, *Science* **336**, 887 (2012).
  - [9] D. N. Matsukevich and A. Kuzmich, *Science* **306**, 663 (2004).
  - [10] Y. A. Chen *et al.*, *Nat. Phys.* **4**, 103 (2007).
  - [11] J. Simon, H. Tanji, S. Ghosh, and V. Vuletic, *Nat. Phys.* **3**, 765 (2007).
  - [12] D. N. Matsukevich *et al.*, *Phys. Rev. Lett.* **96**, 030405 (2006).
  - [13] A. G. Radnaev *et al.*, *Nat. Phys.* **6**, 894 (2010).
  - [14] Y. O. Dudin *et al.*, *Phys. Rev. Lett.* **105**, 260502 (2010).
  - [15] Y. O. Dudin, R. Zhao, T. A. B. Kennedy, and A. Kuzmich, *Phys. Rev. A* **81**, 041805(R) (2010).
  - [16] U. Schnorrberger *et al.*, *Phys. Rev. Lett.* **103**, 033003 (2009).
  - [17] J. J. Longdell, E. Fraval, M. J. Sellars, and N. B. Manson, *Phys. Rev. Lett.* **95**, 063601 (2005).
  - [18] S. Kuhr *et al.*, *Phys. Rev. A* **72**, 023406 (2005).
  - [19] Y. O. Dudin *et al.*, *Phys. Rev. Lett.* **103**, 020505 (2009).
  - [20] N. Lundblad, M. Schlosser, and J. V. Porto, *Phys. Rev. A* **81**, 049904(E) (2010).
  - [21] S. J. M. Kuppens, K. L. Corwin, K. W. Miller, T. E. Chupp, and C. E. Wieman, *Phys. Rev. A* **62**, 013406 (2000).
  - [22] A. Derevianko, *Phys. Rev. A* **81**, 051606(R) (2010).
  - [23] L. Viola and S. Lloyd, *Phys. Rev. A* **58**, 2733 (1998).
  - [24] M. J. Biercuk *et al.*, *Nature (London)* **458**, 996 (2009).
  - [25] Y. Sagi, I. Almog, and N. Davidson, *Phys. Rev. Lett.* **105**, 053201 (2010).
  - [26] L. Vandersypen and I. Chuang, *Rev. Mod. Phys.* **76**, 1037 (2004).
  - [27] D. J. Szwer *et al.*, *J. Phys. B* **44**, 025501 (2011).
  - [28] A. Ajoy, G. A. Alvarez, and D. Suter, *Phys. Rev. A* **83**, 032303 (2011).
  - [29] J. Bylander *et al.*, *Nat. Phys.* **7**, 565 (2011).
  - [30] S. Meiboom and D. Gill, *Rev. Sci. Instrum.* **29**, 688 (1958).